Solving the triharmonic equation over multi-patch planar domains using isogeometric analysis

2 authors:

Mario Kapl
Fachhochschule Kärnten
33 PUBLICATIONS **248** CITATIONS

SEE PROFILE

Vito Vitrih
University of Primorska
39 PUBLICATIONS **258** CITATIONS

SEE PROFILE

Some of the authors of this publication are also working on these related projects:

Automated Mesh Generation for Isogeometric Analysis View project

Solving the triharmonic equation over multi-patch domains using isogeometric analysis

Mario Kapl[a,*], Vito Vitrih[b,c]

[a]*Johann Radon Institute for Computational and Applied Mathematics, Austrian Academy of Sciences, Linz, Austria*
[b]*IAM and FAMNIT, University of Primorska, Koper, Slovenia*
[c]*Institute of Mathematics, Physics and Mechanics, Ljubljana, Slovenia*

Abstract

We present a framework for solving the triharmonic equation over bilinearly parameterized planar multi-patch domains by means of isogeometric analysis. Our approach is based on the construction of a globally C^2-smooth isogeometric spline space which is used as discretization space. The generated C^2-smooth space consists of three different types of isogeometric functions called patch, edge and vertex functions. All functions are entirely local with a small support, and are well-conditioned. The construction of the functions is simple and works uniformly for all multi-patch configurations. While the patch and edge functions are given by a closed form representation, the vertex functions are obtained by solving a small system of linear equations. Several examples demonstrate the potential of our approach for solving the triharmonic equation.

Keywords: isogeometric analysis, triharmonic equation, geometric continuity, C^2-continuity, multi-patch domain
2000 MSC: 65D17, 65N30, 68U07

1. Introduction

In isogeometric analysis (IGA), which was introduced by Hughes et al. [16], standard CAD functions for describing the geometry, such as polynomial splines or NURBS, are also used as test functions in the numerical simulation of partial differential equations (PDEs), cf. [3, 9, 16]. IGA provides the possibility to solve high order PDEs by using standard Galerkin discretization, see e.g. [2, 37], but which requires isogeometric spline spaces of high smoothness. In case of 4-th order PDEs, such as the biharmonic equation [2, 8, 17, 23, 37], the Kirchhoff-Love model of plates and shells [1, 4, 25, 26, 27, 32], or the Cahn-Hilliard equation [11, 12, 29], C^1-smooth isogeometric functions are needed. In order to solve 6-th order PDEs, such as the triharmonic equation [2, 20, 21, 37], the phase-field crystal equation [2, 13], the Kirchhoff plate model based on the Mindlin's gradient elasticity theory

---

*Corresponding author
    Email addresses: `mario.kapl@ricam.oeaw.ac.at` (Mario Kapl), `vito.vitrih@upr.si` (Vito Vitrih)

[33], or the gradient-enhanced continuum damage model [41], even C^2-smooth functions are required. In particular for the case of 6-th order PDEs, these problems have been mainly considered so far for single-patch domains or simple closed surfaces, where the required smoothness of an isogeometric functions is directly obtained by the smoothness of the underlying spline space. In case of multi-patch domains, the construction of C^s-smooth ($s \geq 1$) isogeometric spline spaces defined on multi-patch domains is linked to the concept of geometric continuity of multi-patch surfaces (cf. [15, 34]). More precisely, an isogeometric function is C^s-smooth on a multi-patch domain if and only if its graph surface over the multi-patch domain is G^s-smooth (cf. [14, 23]). The design of C^s-smooth isogeometric spline spaces is the task of recent research, see e.g. [5, 6, 8, 17, 19, 18, 23, 24, 30, 31, 39, 40] for $s = 1$ and e.g. [21, 20, 22, 38] for $s = 2$.

This work focuses on solving the triharmonic equation over bilinearly parameterized planar multi-patch domains by using IGA. To our knowledge this problem was handled for the first time in [20, 21]. There, a basis of the entire space of C^2-smooth isogeometric functions is generated. The construction is based on the concept of minimal determining sets (cf. [28]) for the involved spline coefficients and requires the symbolic solving of a large (global) system of linear equations. Further disadvantages of this approach are the following: The resulting functions which are defined across the common interfaces possess in general large supports along one or more interfaces. The method is restricted to isogeometric spline functions of bidegree (p, p) with $p = 5, 6$ and regularity $r = 2$ within the single patches. Moreover, the presented examples of solving the triharmonic equation were restricted to one particular level of h-refinement.

The present paper improves and extends the approach [20, 21] in several directions. Instead of constructing the entire space of C^2-smooth isogeometric functions, which has a complex structure, a simpler subspace $\mathcal{W}_{0h}$ is generated. The subspace $\mathcal{W}_{0h}$ maintains the full approximation properties of the entire space and is defined as the direct sum of spaces corresponding to the single patches, edges and vertices. For each of these spaces the construction of the basis functions is simple and leads to basis functions which possess small supports, are well-conditioned and can be described by explicit formulae or by the solution of small systems of linear equations. The basis construction of the single spaces is based on and extends the explicit construction in [22], which was introduced for the class of so-called bilinear-like two-patch parameterizations containing the subclass of bilinear two-patch geometries. In addition, the design of the basis functions can be applied for any degree $p \geq 5$ and any regularity $2 \leq r \leq p - 3$ within the single patches, and the construction of the space $\mathcal{W}_{0h}$ works uniformly for all possible multi-patch configurations. In contrast to [20, 21], the triharmonic equation is solved on several bilinearly parameterized multi-patch domains for different levels of h-refinement, where the numerical results show the potential of our approach.

The remainder of the paper is organized as follows. Section 2 introduces the model problem which is studied in this work, i.e., solving the triharmonic equation over bilinear multi-patch domains by means of IGA. This requires the use of a discretization space consisting of globally C^2-smooth isogeometric functions. Section 3 recalls the concept of C^2-smooth isogeometric spline spaces and summarizes the explicit construction [22] for

the case of two patches which serves as a basis for the multi-patch case. In Section 4, we describe the construction of the discretization space for solving the triharmonic equation. This space is a subspace of the entire space of globally C^2-smooth isogeometric spline spaces and is defined as the direct sum of subspaces of three different types called patch, edge and vertex subspaces. The potential of our method for solving the triharmonic equation is demonstrated on the basis of several examples in Section 5, where amongst others the convergence rates and condition numbers obtained under h-refinement are numerically studied. Finally, we conclude the paper.

2. The model problem

We introduce the model problem which will be considered throughout the paper. The goal is to solve a particular sixth-order partial differential equation, namely the triharmonic equation with homogeneous boundary conditions of order 2.

2.1. The triharmonic equation

Let $\Omega = \cup_{\ell=1}^P \Omega^{(\ell)}$ be a planar multi-patch domain. We have to find the function $u : \Omega \to \mathbb{R}$ which solves for $f \in H^0(\Omega)$ the equation

$$\triangle^3 u(\boldsymbol{x}) = -f(\boldsymbol{x}), \quad \boldsymbol{x} \in \Omega, \tag{1}$$

with the boundary conditions

$$u(\boldsymbol{x}) = \frac{\partial u}{\partial \boldsymbol{n}}(\boldsymbol{x}) = \triangle u(\boldsymbol{x}) = 0, \quad \boldsymbol{x} \in \partial\Omega. \tag{2}$$

Using the weak formulation of (1) and (2) we have to find $u \in \mathcal{V}_0$, with

$$\mathcal{V}_0 = \{v \in H^2(\Omega) : \triangle v \in H^1(\Omega) \text{ and } v(\boldsymbol{x}) = \frac{\partial v}{\partial \boldsymbol{n}}(\boldsymbol{x}) = \triangle v(\boldsymbol{x}) = 0 \text{ for } \boldsymbol{x} \in \partial\Omega\},$$

such that

$$\int_\Omega \nabla\left(\triangle u(\boldsymbol{x})\right) \cdot \nabla\left(\triangle v(\boldsymbol{x})\right) \mathrm{d}\boldsymbol{x} = \int_\Omega f(\boldsymbol{x}) v(\boldsymbol{x}) \mathrm{d}\boldsymbol{x}, \tag{3}$$

where $\cdot$ denotes the standard inner product, is satisfied for all $v \in \mathcal{V}_0$, cf. [2, 37]. In order to discretize problem (3) by applying Galerkin projection, a finite dimensional function space $\mathcal{W}_{0h} \subseteq \mathcal{V}_0$ is required. Assume that we have such a space $\mathcal{W}_{0h}$ with a basis $\{w_i\}_{i \in I_h}$, where $I_h = \{1, 2, \ldots, \dim \mathcal{W}_{0h}\}$. Then, we have to find

$$u_h(\boldsymbol{x}) = \sum_{i \in I_h} c_i w_i(\boldsymbol{x}), \quad c_i \in \mathbb{R},$$

which solves the system of equations

$$\int_\Omega \nabla\left(\triangle u_h(\boldsymbol{x})\right) \cdot \nabla\left(\triangle v_h(\boldsymbol{x})\right) \mathrm{d}\boldsymbol{x} = \int_\Omega f(\boldsymbol{x}) v_h(\boldsymbol{x}) \mathrm{d}\boldsymbol{x}$$

for all $v_h \in \mathcal{W}_{0h}$. This results in a system of linear equations

$$S\boldsymbol{c} = \boldsymbol{f}$$

for the unknown coefficients $\boldsymbol{c} = (c_i)_{i \in I_h}$, where the elements of the matrix $S = (s_{i,j})_{i,j \in I_h}$ and the elements of the right-hand side vector $\boldsymbol{f} = (f_i)_{i \in I_h}$ are given by

$$s_{i,j} = \int_\Omega \nabla\left(\triangle w_i(\boldsymbol{x})\right) \cdot \nabla\left(\triangle w_j(\boldsymbol{x})\right) \mathrm{d}\boldsymbol{x} \quad \text{and} \quad f_i = \int_\Omega f(\boldsymbol{x}) w_i(\boldsymbol{x}) \, \mathrm{d}\boldsymbol{x}. \tag{4}$$

In this work, we will follow the isogeometric approach to solve the triharmonic equation. For this purpose, we will construct an isogeometric space $\mathcal{W}_{0h} \subseteq \mathcal{V}_0$ and an associated basis $\{w_i\}_{i \in I_h}$, see Section 4. Beside the fulfillment of the homogeneous boundary conditions (2), the generated basis functions w_i will be C^2-smooth, since C^1-smoothness is not enough to ensure that $w_i \in \mathcal{V}_0$.

2.2. Using the isogeometric approach

We describe the isogeometric approach to compute the elements in (4). We assume that the planar multi-patch domain Ω consists of

- P patches $\Omega^{(\ell)}$, $\ell = 1, 2, \ldots, P$, with $P \in \mathbb{N}$ and $P \geq 2$,

- E non-boundary common edges $\Gamma^{(s)}$, $s = 1, 2, \ldots, E$, and

- V inner and boundary vertices $\boldsymbol{v}^{(\rho)}$ of valency $\bar{\nu}_\rho \geq 3$, $\rho = 1, 2, \ldots, V$. [1]

In addition, we assume that

- the deletion of any vertex does not split Ω into subdomains, whose union would be unconnected,

- all subdomains $\Omega^{(\ell)}$ are mutually disjoint, strictly convex quadrangular patches,

- any two patches $\Omega^{(\ell)}$ and $\Omega^{(\ell')}$ have either an empty intersection, possess exactly one common vertex or share the whole common edge, and

- each patch $\Omega^{(\ell)}$ is parameterized by a bilinear, bijective and regular geometry mapping $\boldsymbol{F}^{(\ell)}$,

$$\boldsymbol{F}^{(\ell)} : [0,1]^2 \to \mathbb{R}^2, \quad \boldsymbol{\xi}^{(\ell)} = (\xi_1^{(\ell)}, \xi_2^{(\ell)}) \mapsto (F_1^{(\ell)}, F_2^{(\ell)}) = \boldsymbol{F}^{(\ell)}(\boldsymbol{\xi}^{(\ell)}), \quad \ell \in \{1, 2, \ldots, P\},$$

such that $\Omega^{(\ell)} = \boldsymbol{F}^{(\ell)}([0,1]^2)$, see Fig. 1.

Let $J^{(\ell)}$ be the Jacobian of $\boldsymbol{F}^{(\ell)}$ and let

$$N^{(\ell)}(\boldsymbol{\xi}^{(\ell)}) = \left(J^{(\ell)}(\boldsymbol{\xi}^{(\ell)})\right)^{-T} \left(J^{(\ell)}(\boldsymbol{\xi}^{(\ell)})\right)^{-1} |\det J^{(\ell)}(\boldsymbol{\xi}^{(\ell)})|.$$

---

[1] In this work, a boundary vertex of valency two is not considered as a vertex $\boldsymbol{v}^{(\rho)}$.
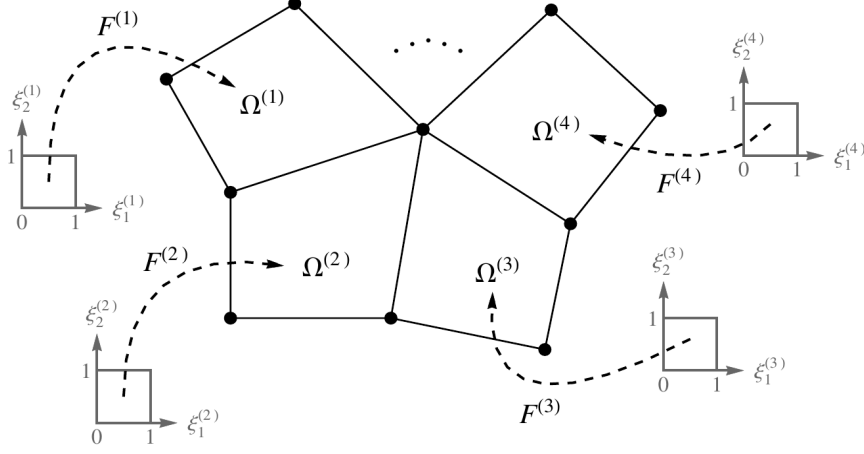
Figure 1: The multi-patch domain $\Omega = \cup_{\ell=1}^{P} \Omega^{(\ell)}$ with the corresponding geometry mappings $\boldsymbol{F}^{(\ell)}$, $\ell = 1, 2, \ldots, P$.

Furthermore, let $W_i^{(\ell)} = w_i \circ \boldsymbol{F}^{(\ell)}$, $i \in I_h$. Then, we compute the elements in (4) patch-wise by

$$s_{i,j} = \sum_{\ell=1}^{P} s_{i,j}^{(\ell)} \quad \text{and} \quad f_i = \sum_{\ell=1}^{P} f_i^{(\ell)},$$

where

$$s_{i,j}^{(\ell)} = \int_{[0,1]^2} \nabla \left(\frac{1}{|\det J^{(\ell)}(\boldsymbol{\xi}^{(\ell)})|} \nabla \cdot \left(N^{(\ell)}(\boldsymbol{\xi}^{(\ell)}) \nabla W_i^{(\ell)}(\boldsymbol{\xi}^{(\ell)}) \right) \right) \cdot \\ \left(N^{(\ell)}(\boldsymbol{\xi}^{(\ell)}) \nabla \left(\frac{1}{|\det J^{(\ell)}(\boldsymbol{\xi}^{(\ell)})|} \nabla \cdot \left(N^{(\ell)}(\boldsymbol{\xi}^{(\ell)}) \nabla W_j^{(\ell)}(\boldsymbol{\xi}^{(\ell)}) \right) \right) \right) \, \mathrm{d}\boldsymbol{\xi}^{(\ell)},$$

and

$$f_i^{(\ell)} = \int_{[0,1]^2} f(\boldsymbol{F}^{(\ell)}(\boldsymbol{\xi}^{(\ell)})) W_i^{(\ell)}(\boldsymbol{\xi}^{(\ell)}) |\det J^{(\ell)}(\boldsymbol{\xi}^{(\ell)})| \, \mathrm{d}\boldsymbol{\xi}^{(\ell)},$$

cf. [2, 21].

3. C^2-smooth isogeometric spline spaces

In Section 4, the isogeometric discretization space $\mathcal{W}_{0h}$ will be generated as a subspace of the space of C^2-smooth isogeometric spline functions on Ω. Before, we recall the concept of C^2-smooth isogeometric spline spaces, cf. [20, 22], and adapt the notations appropriately.

3.1. The space of C^2-smooth isogeometric spline functions

In order to define the space of C^2-smooth isogeometric spline functions on Ω, we need some additional definitions and notations. Let $p \geq 5$, $2 \leq r \leq p - 3$, $k \in \mathbb{N}_0$, and $h = \frac{1}{k+1}$.

We denote by $\mathcal{S}_h^{p,r}([0,1])$ the univariate spline space on the interval $[0,1]$ of degree p and regularity C^r possessing the open knot vector

$$(\underbrace{0,0,\ldots,0}_{(p+1)-\text{times}},\underbrace{\tau_1,\tau_1,\ldots,\tau_1}_{(p-r)-\text{times}},\underbrace{\tau_2,\tau_2,\ldots,\tau_2}_{(p-r)-\text{times}},\ldots,\underbrace{\tau_k,\tau_k,\ldots,\tau_k}_{(p-r)-\text{times}},\underbrace{1,1,\ldots,1}_{(p+1)-\text{times}}),$$

where the k different inner knots τ_j, $j \in \{1,2,\ldots,k\}$, are equally distributed, i.e., $\tau_j = \frac{j}{k+1} = jh$. Let $N_i^{p,r}$, $i = 0,1,\ldots,p+k(p-r)$, be the B-splines of the spline space $\mathcal{S}_h^{p,r}([0,1])$, and let $\mathcal{S}_h^{p,r}([0,1]^2)$ be the bivariate tensor-product spline space on the unit-square $[0,1]^2$ spanned by the B-splines $N_{i,j}^{p,r} = N_i^{p,r} N_j^{p,r}$, $i,j = 0,1,\ldots,p+k(p-r)$. Note that h is the mesh-size of the spline spaces $\mathcal{S}_h^{p,r}([0,1])$ and $\mathcal{S}_h^{p,r}([0,1]^2)$. Below, we assume that the number of inner knots satisfies $k \geq \frac{9-p}{p-r-2}$, which implies $h \leq \frac{p-r-2}{7-r}$.

Recall that the geometry mappings $\boldsymbol{F}^{(\ell)}$, $\ell = 1,2,\ldots,P$, are bilinear parameterizations, which also implies that $\boldsymbol{F}^{(\ell)} \in \mathcal{S}_h^{p,r}([0,1]^2) \times \mathcal{S}_h^{p,r}([0,1]^2)$. Then, the space of globally C^2-smooth isogeometric spline functions on Ω (with respect to the spline space $\mathcal{S}_h^{p,r}([0,1]^2)$) is defined as

$$\mathcal{V}_h = \left\{ \phi \in C^2(\Omega) : \ \phi|_{\Omega^{(\ell)}} \in \mathcal{S}_h^{p,r}([0,1]^2) \circ (\boldsymbol{F}^{(\ell)})^{-1}, \ \ell \in \{1,2,\ldots,P\} \right\}.$$

The graph surface $\boldsymbol{\Sigma} : [0,1]^2 \to \Omega \times \mathbb{R}$ of an isogeometric function $\phi \in \mathcal{V}_h$ is given patch-wise by the graph surface patches

$$\boldsymbol{\Sigma}^{(\ell)}(\boldsymbol{\xi}^{(\ell)}) = \left(\boldsymbol{F}^{(\ell)}(\boldsymbol{\xi}^{(\ell)}), g^{(\ell)}(\boldsymbol{\xi}^{(\ell)}) \right)^T, \quad g^{(\ell)} \in \mathcal{S}_h^{p,r}([0,1]^2), \quad \ell = 1,2,\ldots,P,$$

with

$$g^{(\ell)}(\boldsymbol{\xi}^{(\ell)}) = \phi \circ \boldsymbol{F}^{(\ell)}(\boldsymbol{\xi}^{(\ell)}) = \sum_{i=0}^{p+k(p-r)} \sum_{j=0}^{p+k(p-r)} d_{i,j}^{(\ell)} N_{i,j}^{p,r}(\boldsymbol{\xi}^{(\ell)}), \quad d_{i,j}^{(\ell)} \in \mathbb{R}. \tag{5}$$

The functions in $\mathcal{V}_h$ can be characterized by using the concept of geometric continuity (cf. [14, 23]): *An isogeometric function ϕ belongs to the space $\mathcal{V}_h$ if and only if for all neighboring patches $\Omega^{(\ell)}$ and $\Omega^{(\ell')}$ sharing an interface $\Gamma^{(s)} = \Omega^{(\ell)} \cap \Omega^{(\ell')}$ (where $s \in \{1,2,\ldots,E\}$), the two graph surface patches $\boldsymbol{\Sigma}^{(\ell)}$ and $\boldsymbol{\Sigma}^{(\ell')}$ meet at the common interface $\Gamma^{(s)}$ with G^2 continuity.* Since the geometry mappings $\boldsymbol{F}^{(\ell)}$ and $\boldsymbol{F}^{(\ell')}$ are given in advance, the G^2 continuity conditions for the graph surface patches $\boldsymbol{\Sigma}^{(\ell)}$ and $\boldsymbol{\Sigma}^{(\ell')}$ lead to conditions for the spline functions $g^{(\ell)}$ and $g^{(\ell')}$, which determine again linear constraints on the spline coefficients $d_{i,j}^{(\ell)}$ and $d_{i,j}^{(\ell')}$. These conditions were studied in [22] for the class of so-called bilinear-like G^2 geometries, which includes the class of bilinearly parameterized geometries. Let us shortly recall the conditions for the two neighboring patches $\Omega^{(\ell)}$ and $\Omega^{(\ell')}$. For the sake of simplicity, we can always reparameterize (if needed) the two geometry mappings $\boldsymbol{F}^{(\ell)}$ and $\boldsymbol{F}^{(\ell')}$ to have the situation as given in Fig. 2, i.e.,

$$\boldsymbol{F}^{(\ell)}(0,\xi) = \boldsymbol{F}^{(\ell')}(0,\xi), \quad \xi = \xi_2^{(\ell)} = \xi_2^{(\ell')} \in [0,1].$$

To simplify the notation, let us denote the common interface $\Gamma^{(s)}$ in this section by Γ and let

$$\bar{\alpha}_\Gamma^{(\tau)}(\xi) = \det[D_{\xi_1^{(\tau)}}\boldsymbol{F}^{(\tau)}(0,\xi), D_\xi \boldsymbol{F}^{(\tau)}(0,\xi)], \ \alpha_\Gamma^{(\tau)}(\xi) = \gamma_1(\xi)\bar{\alpha}_\Gamma^{(\tau)}(\xi), \ \widehat{\alpha}_\Gamma^{(\tau)}(\xi) = \gamma_2(\xi)\bar{\alpha}_\Gamma^{(\tau)}(\xi),$$
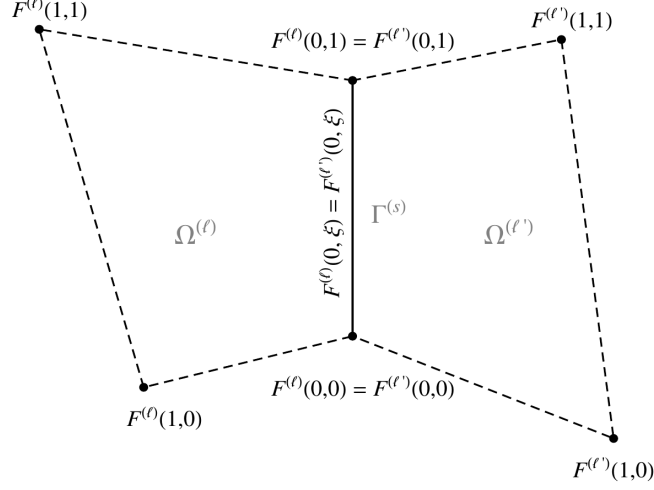
Figure 2: Considering two neighboring patches $\Omega^{(\ell)}$ and $\Omega^{(\ell)}$, we can always assume (without loss of generality) that the two corresponding geometry mappings $\boldsymbol{F}^{(\ell)}$ and $\boldsymbol{F}^{(\ell')}$ are parameterized as shown.

for $\tau \in \{\ell, \ell'\}$ and

$$\bar{\beta}_\Gamma(\xi) = \det[D_{\xi_1^{(\ell)}} \boldsymbol{F}^{(\ell)}(0, \xi), D_{\xi_1^{(\ell')}} \boldsymbol{F}^{(\ell')}(0, \xi)], \quad \beta_\Gamma(\xi) = \gamma_1(\xi) \bar{\beta}_\Gamma(\xi)$$

for $\gamma_i : [0, 1] \to \mathbb{R}$, $i = 1, 2$. Note that $\bar{\alpha}_\Gamma^{(\ell)}$ and $\bar{\alpha}_\Gamma^{(\ell')}$ are linear polynomials with $\bar{\alpha}_\Gamma^{(\ell)} < 0$ and $\bar{\alpha}_\Gamma^{(\ell')} > 0$, respectively, and $\bar{\beta}_\Gamma$ is a quadratic polynomial. We can write the function β_Γ also as

$$\beta_\Gamma(\xi) = \alpha_\Gamma^{(\ell)}(\xi) \beta_\Gamma^{(\ell')}(\xi) - \alpha_\Gamma^{(\ell')}(\xi) \beta_\Gamma^{(\ell)}(\xi),$$

where $\beta_\Gamma^{(\ell)}, \beta_\Gamma^{(\ell')} : [0, 1] \to \mathbb{R}$ are given as

$$\beta_\Gamma^{(\tau)}(\xi) = \frac{D_{\xi_1^{(\tau)}} \boldsymbol{F}^{(\tau)}(0, \xi) \cdot D_\xi \boldsymbol{F}^{(\tau)}(0, \xi)}{||D_\xi \boldsymbol{F}^{(\tau)}(0, \xi)||^2}, \quad \tau \in \{\ell, \ell'\}.$$

Moreover let

$$\eta_\Gamma(\xi) = 2\gamma_2(\xi)(\alpha_\Gamma^{(\ell)})'(\xi)\alpha_\Gamma^{(\ell')}(\xi)\beta_\Gamma(\xi),$$

$$\theta_\Gamma(\xi) = 2\gamma_2(\xi)\left(\alpha_\Gamma^{(\ell)}(\xi)(\beta_\Gamma^{(\ell)})'(\xi) - (\alpha_\Gamma^{(\ell)})'(\xi)\beta_\Gamma^{(\ell)}(\xi)\right)\alpha_\Gamma^{(\ell')}(\xi)\beta_\Gamma(\xi).$$

Then, we have: $\phi \in \mathcal{V}_h$ if and only if

$$g^{(\ell)}(0, \xi) = g^{(\ell')}(0, \xi), \tag{6}$$

$$\alpha_\Gamma^{(\ell')}(\xi)D_{\xi_1^{(\ell)}}g^{(\ell)}(0, \xi) - \alpha_\Gamma^{(\ell)}(\xi)D_{\xi_1^{(\ell')}}g^{(\ell')}(0, \xi) + \beta_\Gamma(\xi)D_\xi g^{(\ell)}(0, \xi) = 0, \tag{7}$$

and

$$\widehat{\alpha}_\Gamma^{(\ell)}(\xi)w_\Gamma(\xi) + \eta_\Gamma(\xi)D_{\xi_1^{(\ell)}}g^{(\ell)}(0, \xi) + \theta_\Gamma(\xi)D_\xi g^{(\ell)}(0, \xi) = 0, \tag{8}$$

7

where

$$w_\Gamma(\xi) = (\alpha_\Gamma^{(\ell)}(\xi))^2 D_{\xi_1^{(\ell')}\xi_1^{(\ell')}} g^{(\ell')}(0,\xi) - ((\alpha_\Gamma^{(\ell')}(\xi))^2 D_{\xi_1^{(\ell)}\xi_1^{(\ell)}} g^{(\ell)}(0,\xi)$$

$$+ 2\alpha_\Gamma^{(\ell')}(\xi)\beta_\Gamma(\xi) D_{\xi_1^{(\ell)}\xi} g^{(\ell)}(0,\xi) + (\beta_\Gamma(\xi))^2 D_{\xi\xi} g^{(\ell)}(0,\xi)).$$

Note that condition (6) guarantees that ϕ is C^0-smooth, condition (7) additionally ensures that ϕ is C^1-smooth, and condition (8) finally implies that ϕ is C^2-smooth.

Remark 1. Below, we choose $\gamma_2(\xi) = 1$, implying $\widehat{\alpha}^{(\tau)} = \bar{\alpha}^{(\tau)}$, $\tau \in \{\ell, \ell'\}$. In addition, we select $\gamma_1(\xi) = c_1 \in \mathbb{R}$ such that

$$||\alpha_\Gamma^{(\ell)} + 1||_{L^2}^2 + ||\alpha_\Gamma^{(\ell')} - 1||_{L^2}^2$$

is minimized, cf. [18].

3.2. The two-patch case

In this subsection we restrict ourselves to the two-patch case $\Omega = \Omega^{(\ell)} \cup \Omega^{(\ell')}$ for two neighboring patches $\Omega^{(\ell)}$ and $\Omega^{(\ell')}$ having the common interface $\Gamma^{(s)} = \Omega^{(\ell)} \cap \Omega^{(\ell')}$. Without loss of generality, we can assume that the two geometry mappings $\boldsymbol{F}^{(\ell)}$ and $\boldsymbol{F}^{(\ell')}$ are parameterized as in Fig. 2. We recall now the construction of a C^2-smooth isogeometric spline space $\widetilde{\mathcal{W}}_h \subseteq \mathcal{V}_h$, which was described in [22], by using now adapted notations. The subspace $\widetilde{\mathcal{W}}_h$ is advantageous compared to the entire space $\mathcal{V}_h$, since its basis construction is simpler and works uniformly for all possible configurations. In addition, it was numerically demonstrated in [22] that already the subspace $\widetilde{\mathcal{W}}_h$ possesses optimal approximation properties. For a detailed investigation of the spaces $\widetilde{\mathcal{W}}_h$ and $\mathcal{V}_h$ we refer to [22].

The space $\widetilde{\mathcal{W}}_h$ is the direct sum of three subspaces, i.e.,

$$\widetilde{\mathcal{W}}_h = \widetilde{\mathcal{W}}_{h;\Omega^{(\ell)}} \oplus \widetilde{\mathcal{W}}_{h;\Omega^{(\ell')}} \oplus \widetilde{\mathcal{W}}_{h;\Gamma^{(s)}}.$$

The subspaces $\widetilde{\mathcal{W}}_{h;\Omega^{(\ell)}}$ and $\widetilde{\mathcal{W}}_{h;\Omega^{(\ell')}}$ are given by

$$\widetilde{\mathcal{W}}_{h;\Omega^{(\tau)}} = \text{span}\{\widetilde{\phi}_{\Omega^{(\tau)};i,j}|\ i = 3, 4, \ldots, p + k(p - r),\ j = 0, 1, \ldots, p + k(p - r)\}, \quad \tau \in \{\ell, \ell'\},$$

with the functions

$$\widetilde{\phi}_{\Omega^{(\tau)};i,j}(\boldsymbol{x}) = \begin{cases} (N_{i,j}^{p,r} \circ (\boldsymbol{F}^{(\tau)})^{-1})(\boldsymbol{x}) & \text{if } \boldsymbol{x} \in \Omega^{(\tau)}, \\ 0 & \text{if } \boldsymbol{x} \in \Omega \backslash \Omega^{(\ell)}. \end{cases} \tag{9}$$

In order to define the subspace $\widetilde{\mathcal{W}}_{h;\Gamma^{(s)}}$, we need some additional definitions. Let

$$M_0(\xi) = \sum_{i=0}^{2} N_i^{p,r}(\xi),\ M_1(\xi) = \frac{h}{p}\left(N_1^{p,r}(\xi) + 2N_2^{p,r}(\xi)\right),\ M_2(\xi) = \frac{h^2}{p(p-1)}N_2^{p,r}(\xi), \tag{10}$$

8

and let

$$n_0 = \dim\left(\mathcal{S}_h^{p,r+2}([0,1])\right), \ n_1 = \dim\left(\mathcal{S}_h^{p-d_\alpha,r+1}([0,1])\right), \ n_2 = \dim\left(\mathcal{S}_h^{p-2d_\alpha,r}([0,1])\right),$$

where $d_\alpha = \max\left(\deg(\alpha_{\Gamma^{(s)}}^{(\ell)}), \deg(\alpha_{\Gamma^{(s)}}^{(\ell')})\right) \in \{0,1\}$. The space $\widetilde{\mathcal{W}}_{h;\Gamma^{(s)}}$ is given by

$$\widetilde{\mathcal{W}}_{h;\Gamma^{(s)}} = \operatorname{span}\{\widetilde{\phi}_{\Gamma^{(s)};i,j}| \ i = 0,1,2, \ j = 0,1,\ldots,n_i - 1\},$$

with the functions

$$\widetilde{\phi}_{\Gamma^{(s)};i,j}(\boldsymbol{x}) = \begin{cases} (g_{\Gamma^{(s)};i,j}^{(\ell)} \circ (\boldsymbol{F}^{(\ell)})^{-1})(\boldsymbol{x}) & \text{if } \boldsymbol{x} \in \Omega^{(\ell)}, \\ (g_{\Gamma^{(s)};i,j}^{(\ell')} \circ (\boldsymbol{F}^{(\ell')})^{-1})(\boldsymbol{x}) & \text{if } \boldsymbol{x} \in \Omega^{(\ell')}, \end{cases} \tag{11}$$

where

$$
\begin{aligned}
g_{\Gamma^{(s)};0,j}^{(\tau)}(\boldsymbol{\xi}^{(\tau)}) =\ & N_j^{p,r+2}(\xi_2^{(\tau)})M_0(\xi_1^{(\tau)}) + \beta_{\Gamma^{(s)}}^{(\tau)}(\xi_2^{(\tau)})(N_j^{p,r+2})'(\xi_2^{(\tau)})M_1(\xi_1^{(\tau)}) \\
& + \left(\beta_{\Gamma^{(s)}}^{(\tau)}(\xi_2^{(\tau)})\right)^2 (N_j^{p,r+2})''(\xi_2^{(\tau)})M_2(\xi_1^{(\tau)}), \\
g_{\Gamma^{(s)};1,j}^{(\tau)}(\boldsymbol{\xi}^{(\tau)}) =\ & \frac{p}{h}\left(\alpha_{\Gamma^{(s)}}^{(\tau)}(\xi_2^{(\tau)})N_j^{p-d_\alpha,r+1}(\xi_2^{(\tau)})M_1(\xi_1^{(\tau)})\right. \\
& \left. + 2\,\alpha_{\Gamma^{(s)}}^{(\tau)}(\xi_2^{(\tau)})\beta_{\Gamma^{(s)}}^{(\tau)}(\xi_2^{(\tau)})(N_j^{p-d_\alpha,r+1})'(\xi_2^{(\tau)})M_2(\xi_1^{(\tau)})\right), \\
g_{\Gamma^{(s)};2,j}^{(\tau)}(\boldsymbol{\xi}^{(\tau)}) =\ & \frac{p(p-1)}{h^2}\left(\alpha_{\Gamma^{(s)}}^{(\tau)}(\xi_2^{(\tau)})\right)^2 N_j^{p-2d_\alpha,r}(\xi_2^{(\tau)})M_2(\xi_1^{(\tau)}),
\end{aligned}
\tag{12}
$$

for $\tau \in \{\ell, \ell'\}$.

Remark 2. The functions in (12) are scaled in comparison to the ones in [22].

The following proposition gives an estimate for the support of the function $g_{\Gamma^{(s)};i,j}^{(\tau)}$, and will be needed later.

Proposition 1. *Let* $d = \dim(\mathcal{S}_h^{p,r}([0,1])) = p + k(p-r) + 1$. *The functions* $g_{\Gamma^{(s)};i,j}^{(\tau)}$, $j = 0,1,\ldots,n_i - 1$, $i = 0,1,2$, $\tau \in \{\ell, \ell'\}$, *can be represented as*

$$g_{\Gamma^{(s)};i,j}^{(\tau)}(\boldsymbol{\xi}^{(\tau)}) = \sum_{m=0}^{2} \sum_{n=\max(0,i+j-m)}^{\min(d-1,d-n_i+j-i+m)} d_{\Gamma^{(s)};m,n}^{(\tau)} N_{m,n}^{p,r}(\boldsymbol{\xi}^{(\tau)}), \qquad d_{\Gamma^{(s)};m,n}^{(\tau)} \in \mathbb{R}. \tag{13}$$

Proof. See Appendix A. $\square$

In the next section we will use the C^2-smooth isogeometric functions for the two-patch case to construct a C^2-smooth isogeometric spline space $\mathcal{W}_{0h}$ for the multi-patch case.

4. C^2-smooth discretization space $\mathcal{W}_{0h}$

A C^2-smooth discretization space $\mathcal{W}_{0h}$ will be constructed which can be used for solving the triharmonic equation (1) with homogeneous boundary conditions (2), see Section 5. This space will be a subspace of $\mathcal{V}_h$ or more precisely of the space $\mathcal{V}_{0h}$ given by

$$\mathcal{V}_{0h} = \{\phi \in \mathcal{V}_h : \; \phi(\boldsymbol{x}) = \frac{\partial \phi}{\partial \boldsymbol{n}}(\boldsymbol{x}) = \triangle \phi(\boldsymbol{x}) = 0, \quad \boldsymbol{x} \in \partial\Omega\},$$

which contains all C^2-smooth functions on Ω fulfilling the homogeneous boundary conditions (2).

4.1. Structure of the space $\mathcal{W}_{0h}$

The discretization space $\mathcal{W}_{0h}$ is the direct sum of smaller subspaces corresponding to the single patches $\Omega^{(\ell)}$, edges $\Gamma^{(s)}$ and vertices $\boldsymbol{v}^{(\rho)}$, i.e.,

$$\mathcal{W}_{0h} = \left(\bigoplus_{\ell=1}^{P} \mathcal{W}_{0h;\Omega^{(\ell)}} \right) \oplus \left(\bigoplus_{s=1}^{E} \mathcal{W}_{0h;\Gamma^{(s)}} \right) \oplus \left(\bigoplus_{\rho=1}^{V} \mathcal{W}_{0h;\boldsymbol{v}^{(\rho)}} \right). \tag{14}$$

This decomposition is a common strategy to generate smooth spline spaces, e.g. [18, 20]. The construction of the single subspaces will be presented in the following subsections and will be based on functions from the subspaces $\widetilde{\mathcal{W}}_{h;\Omega^{(\ell)}}$ and $\widetilde{\mathcal{W}}_{h;\Gamma^{(s)}}$ for the two-patch case in Section 3.2.

4.2. The patch subspace $\mathcal{W}_{0h;\Omega^{(\ell)}}$

Let $\ell \in \{1, 2, \ldots, P\}$. We denote by $\phi_{\Omega^{(\ell)};i,j} : \Omega \to \mathbb{R}$, $i, j = 3, 4, \ldots, p + k(p - r) - 3$, the functions

$$\phi_{\Omega^{(\ell)};i,j}(\boldsymbol{x}) = \begin{cases} \widetilde{\phi}_{\Omega^{(\ell)};i,j}(\boldsymbol{x}) & \text{if } \boldsymbol{x} \in \Omega^{(\ell)}, \\ 0 & otherwise, \end{cases} \tag{15}$$

with $\widetilde{\phi}_{\Omega^{(\ell)};i,j}$ given in (9). Then, we define the patch subspace $\mathcal{W}_{0h;\Omega^{(\ell)}}$ as

$$\mathcal{W}_{0h;\Omega^{(\ell)}} = \mathrm{span}\{\phi_{\Omega^{(\ell)};i,j} \,|\, i, j = 3, 4, \ldots, p + k(p - r) - 3\}.$$

Lemma 1. *We have*

$$\mathcal{W}_{0h;\Omega^{(\ell)}} \subseteq \mathcal{V}_{0h}.$$

PROOF. By (15), the functions $\phi_{\Omega^{(\ell)};i,j}$, $i, j = 3, 4, \ldots, p + k(p - r) - 3$, possess a support

$$\mathrm{supp}(\phi_{\Omega^{(\ell)};i,j}) \subseteq \Omega^{(\ell)},$$

they are clearly C^2-smooth on $\Omega^{(\ell)}$, and have vanishing values, gradients and Hessians on $\partial\Omega^{(\ell)}$. This implies that $\phi_{\Omega^{(\ell)};i,j} \in \mathcal{V}_{0h}$. $\qquad\square$

4.3. The edge subspace $\mathcal{W}_{0h;\Gamma^{(s)}}$

Let $s \in \{1, 2, \ldots, E\}$ and let $\ell, \ell' \in \{1, 2, \ldots, P\}$, $\ell \neq \ell'$, be the corresponding indices of the two patches such that $\Gamma^{(s)} = \Omega^{(\ell)} \cap \Omega^{(\ell')}$. Without loss of generality, we can assume that the two geometry mappings $\boldsymbol{F}^{(\ell)}$ and $\boldsymbol{F}^{(\ell')}$ are parameterized as in Fig. 2. Otherwise, suitable linear reparameterizations of the two patches can be applied to fulfill this situation.

We denote by $\phi_{\Gamma^{(s)};i,j} : \Omega \to \mathbb{R}$, $i = 0, 1, 2$, $j = 0, 1, \ldots, n_i - 1$, the functions

$$\phi_{\Gamma^{(s)};i,j}(\boldsymbol{x}) = \begin{cases} \widetilde{\phi}_{\Gamma^{(s)};i,j}(\boldsymbol{x}) & \text{if } \boldsymbol{x} \in \Omega^{(\ell)} \cup \Omega^{(\ell')}, \\ 0 & otherwise, \end{cases} \tag{16}$$

with $\widetilde{\phi}_{\Gamma^{(s)};i,j}$ given in (11). Then, the edge subspace $\mathcal{W}_{0h;\Gamma^{(s)}}$ is defined as

$$\mathcal{W}_{0h;\Gamma^{(s)}} = \text{span}\{\phi_{\Gamma^{(s)};i,j} \mid j = 5 - i, 6 - i, \ldots, n_i + i - 6; \ i = 0, 1, 2\}.$$

Lemma 2. *It holds that*

$$\mathcal{W}_{0h;\Gamma^{(s)}} \subseteq \mathcal{V}_{0h}.$$

Proof. Let $i = 0, 1, 2$ and $j = 5 - i, 6 - i, \ldots, n_i + i - 6$. By (16), the functions $\phi_{\Gamma^{(s)};i,j}$ possess a support

$$\text{supp}(\phi_{\Gamma^{(s)};i,j}) \subseteq \Omega^{(\ell)} \cup \Omega^{(\ell')}.$$

Furthermore, it was shown in [22], that the functions $\phi_{\Gamma^{(s)};i,j}$ are C^2-smooth on $\Omega^{(\ell)} \cup \Omega^{(\ell')}$. Since Proposition 1 ensures that the functions $\phi_{\Gamma^{(s)};i,j}$ have vanishing values, gradients and Hessians on $\partial(\Omega^{(\ell)} \cup \Omega^{(\ell')})$, we obtain $\phi_{\Gamma^{(s)};i,j} \in \mathcal{V}_{0h}$. $\qquad\square$

4.4. The vertex subspace $\mathcal{W}_{0h;\boldsymbol{v}^{(\rho)}}$

We consider an inner or boundary vertex $\boldsymbol{v}^{(\rho)}$, $\rho \in \{1, 2, \ldots, V\}$, possessing the valency $\bar{\nu}_\rho \geq 3$. We define ν_ρ as

$$\nu_\rho = \begin{cases} \bar{\nu}_\rho, & \text{if } \boldsymbol{v}^{(\rho)} \text{ is an inner vertex}, \\ \bar{\nu}_\rho - 1, & \text{if } \boldsymbol{v}^{(\rho)} \text{ is a boundary vertex}. \end{cases}$$

For the sake of simplicity, we relabel the patches containing the vertex $\boldsymbol{v}^{(\rho)}$ in counterclockwise order by $\Omega^{(0)}, \Omega^{(1)}, \ldots, \Omega^{(\nu_\rho - 1)}$. Furthermore, we assume without loss of generality that the corresponding geometry mappings $\boldsymbol{F}^{(\ell)}$, $\ell = 0, 1, \ldots, \nu_\rho - 1$, are parameterized as shown in Fig. 3, which assures that

$$\boldsymbol{F}^{(0)}(\boldsymbol{0}) = \boldsymbol{F}^{(1)}(\boldsymbol{0}) = \cdots = \boldsymbol{F}^{(\nu_\rho - 1)}(\boldsymbol{0}) = \boldsymbol{v}^{(\rho)}.$$

Moreover, we relabel the common interface of every two-patch subdomain $\Omega^{(\ell)} \cup \Omega^{(\ell+1)}$, $\ell = 0, 1, \ldots, \nu_\rho - 1$, by $\Gamma^{(\ell+1)}$. In case of an inner vertex $\boldsymbol{v}^{(\rho)}$, we consider the upper index ℓ of $\Omega^{(\ell)}$ and $\Gamma^{(\ell)}$ modulo ν_ρ, and in case of a boundary vertex $\boldsymbol{v}^{(\rho)}$, we denote by $\Gamma^{(0)}$ the edge of $\Omega^{(0)}$ corresponding to $\boldsymbol{F}^{(0)}([0, 1] \times \{0\})$, and by $\Gamma^{(\nu_\rho)}$ the edge of $\Omega^{(\nu_\rho - 1)}$ corresponding to $\boldsymbol{F}^{(\nu_\rho - 1)}(\{0\} \times [0, 1])$. In addition, we denote by $\bar{\boldsymbol{\xi}}^{(\ell)}$ the pair of parameters $\bar{\boldsymbol{\xi}}^{(\ell)} = (\xi_2^{(\ell)}, \xi_1^{(\ell)})$.
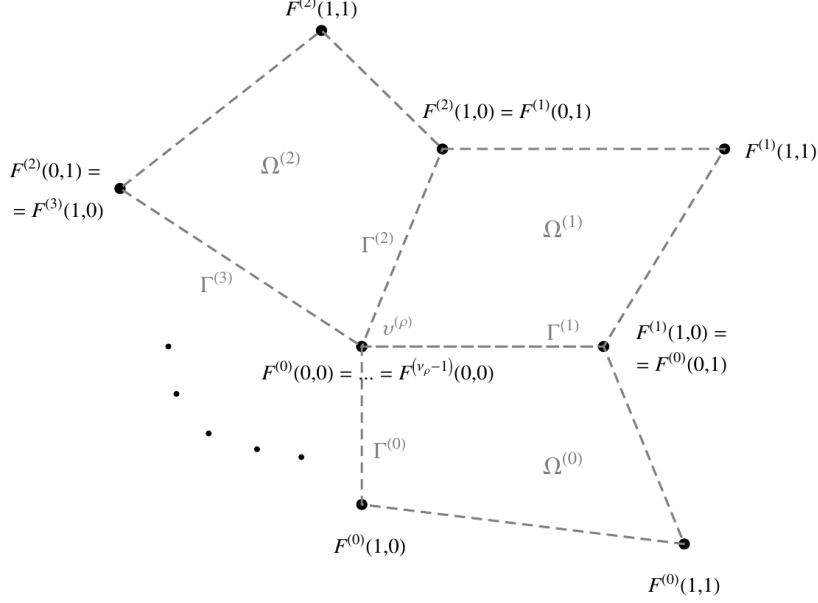
Figure 3: The geometry mappings $\boldsymbol{F}^{(\ell)}$ of the patches $\Omega^{(\ell)}$, $\ell = 0, 1, \ldots, \nu_\rho - 1$, which contain the vertex $\boldsymbol{v}^{(\rho)}$, can be always reparameterized as shown.

The idea is to construct the vertex subspace $\mathcal{W}_{0h;\boldsymbol{v}^{(\rho)}}$ as the space of functions which can be represented by suitable linear combinations of functions $\phi_{\Omega^{(\ell)};i,j}$, $i+j \leq 4$, $0 \leq \ell \leq \nu_\rho - 1$, and of functions $\phi_{\Gamma^{(\ell)};i,j}$, $0 \leq i \leq 2$, $0 \leq j \leq 4-i$, $0 \leq \ell \leq \bar{\nu}_\rho - 1$. Note that none of these functions are contained in any of the spaces $\mathcal{W}_{0h;\Omega^{(\ell)}}$ and $\mathcal{W}_{0h;\Gamma^{(s)}}$. Recall that the functions $\phi_{\Gamma^{(\ell)};i,j}$ are C^2-smooth on the two-patch subdomain $\Omega^{(\ell-1)} \cup \Omega^{(\ell)}$.

For each patch $\Omega^{(\ell)}$, $\ell = 0, 1, \ldots, \nu_\rho - 1$, we define the function $f_\ell : [0,1]^2 \to \mathbb{R}$ as

$$f_\ell(\boldsymbol{\xi}^{(\ell)}) = f_\ell^{\Gamma^{(\ell)}}(\boldsymbol{\xi}^{(\ell)}) + f_\ell^{\Gamma^{(\ell+1)}}(\boldsymbol{\xi}^{(\ell)}) - f_\ell^{\Omega^{(\ell)}}(\boldsymbol{\xi}^{(\ell)}),$$

where the functions $f_\ell^{\Gamma^{(\ell)}}, f_\ell^{\Gamma^{(\ell+1)}}, f_\ell^{\Omega^{(\ell)}} : [0,1]^2 \to \mathbb{R}$ are given by

$$f_\ell^{\Gamma^{(\ell)}}(\boldsymbol{\xi}^{(\ell)}) = \sum_{i=0}^{2} \sum_{j=0}^{4-i} a_{i,j}^{\Gamma^{(\ell)}} \, g_{\Gamma^{(\ell)};i,j}^{(\ell)}(\bar{\boldsymbol{\xi}}^{(\ell)}) + \sum_{j=3}^{4} \sum_{i=0}^{4-j} a_{i,j}^{(\ell)} N_{i,j}^{p,r}(\boldsymbol{\xi}^{(\ell)}),$$

$$f_\ell^{\Gamma^{(\ell+1)}}(\boldsymbol{\xi}^{(\ell)}) = \sum_{i=0}^{2} \sum_{j=0}^{4-i} a_{i,j}^{\Gamma^{(\ell+1)}} \, g_{\Gamma^{(\ell+1)};i,j}^{(\ell)}(\boldsymbol{\xi}^{(\ell)}) + \sum_{i=3}^{4} \sum_{j=0}^{4-i} a_{i,j}^{(\ell)} N_{i,j}^{p,r}(\boldsymbol{\xi}^{(\ell)}),$$

$$f_\ell^{\Omega^{(\ell)}}(\boldsymbol{\xi}^{(\ell)}) = \sum_{i=0}^{4} \sum_{j=0}^{4-i} a_{i,j}^{(\ell)} N_{i,j}^{p,r}(\boldsymbol{\xi}^{(\ell)}),$$

with $a_{i,j}^{\Gamma^{(\ell)}}, a_{i,j}^{\Gamma^{(\ell+1)}}, a_{i,j}^{(\ell)} \in \mathbb{R}$. Furthermore, we define the function $\phi_{\boldsymbol{v}^{(\rho)}} : \Omega \to \mathbb{R}$ as

$$\phi_{\boldsymbol{v}^{(\rho)}}(\boldsymbol{x}) = \begin{cases} (f_\ell \circ (\boldsymbol{F}^{(\ell)})^{-1})(\boldsymbol{x}) & \text{if } \boldsymbol{x} \in \Omega^{(\ell)}, \ \ell = 0, 1, \ldots, \nu_\rho - 1, \\ 0 & \text{otherwise.} \end{cases} \tag{17}$$

The idea for the construction of the function $\phi_{\boldsymbol{v}^{(\rho)}}$ is as follows. On each patch $\Omega^{(\ell)}$, $\ell = 0, 1, \ldots, \nu_\rho - 1$, the function $\phi_{\boldsymbol{v}^{(\rho)}}$ is determined by the spline function f_ℓ, where the sum of the functions $f_\ell^{\Gamma^{(\ell)}}$ and $f_\ell^{\Gamma^{(\ell+1)}}$ should ensure C^2-smoothness across the interfaces $\Gamma^{(\ell)}$ and $\Gamma^{(\ell+1)}$, and the function $f_\ell^{\Omega^{(\ell)}}$ is used to subtract those B-splines $N_{i,j}^{p,r}$ (with respect to the spline space $\mathcal{S}_h^{p,r}([0,1]^2)$), which have been added twice, see Fig. 4.
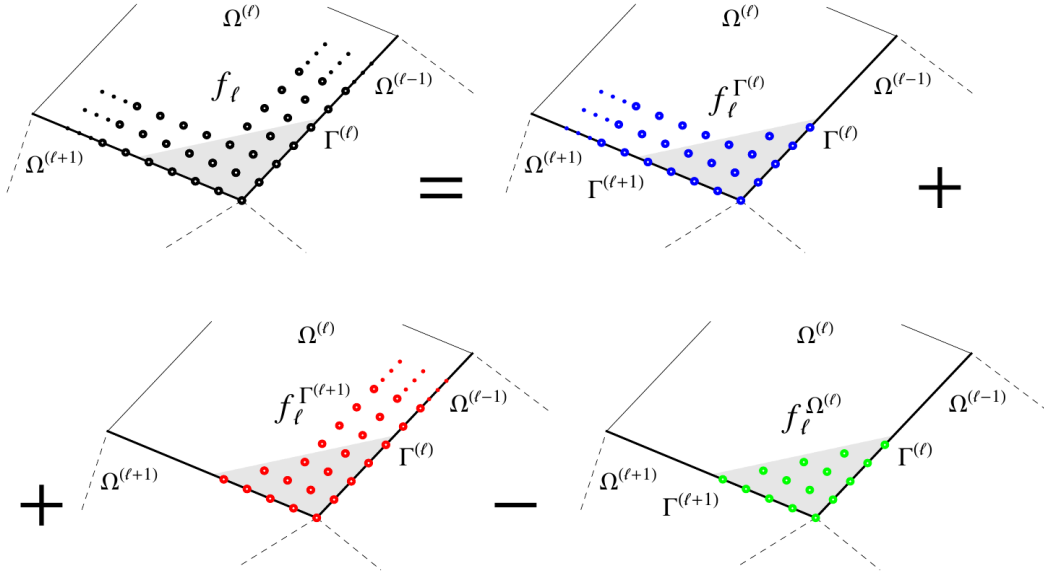
Figure 4: On each patch $\Omega^{(\ell)}$, the function f_ℓ is obtained by summing up the two functions $f_\ell^{\Gamma^{(\ell)}}$ and $f_\ell^{\Gamma^{(\ell+1)}}$ and by subtracting the function $f_\ell^{\Omega^{(\ell)}}$. The non-zero spline coefficients of the single functions are visualized in different colors. To ensure that the function $\phi_{\boldsymbol{v}^{(\rho)}}$ is C^2-smooth on Ω, the values of the corresponding spline control points of the functions $f_\ell^{\Gamma^{(\ell)}}$, $f_\ell^{\Gamma^{(\ell+1)}}$ and $f_\ell^{\Omega^{(\ell)}}$ in the gray regions have to coincide (compare Lemma 3).

Clearly, not any choice of the coefficients $a_{i,j}^{\Gamma^{(\ell)}}$ and $a_{i,j}^{(\ell)}$, $\ell = 0, 1, \ldots, \nu_\rho - 1$, guarantees $\phi_{\boldsymbol{v}^{(\rho)}} \in \mathcal{V}_h$ or as needed in our case even $\phi_{\boldsymbol{v}^{(\rho)}} \in \mathcal{V}_{0h}$. The following lemma characterizes when the function $\phi_{\boldsymbol{v}^{(\rho)}}$ belongs to the space $\mathcal{V}_{0h}$:

Lemma 3. $\phi_{\boldsymbol{v}^{(\rho)}} \in \mathcal{V}_{0h}$ if the corresponding functions $f_\ell^{\Gamma^{(\ell)}}$, $f_\ell^{\Gamma^{(\ell+1)}}$, and $f_\ell^{\Omega^{(\ell)}}$, $\ell = 0, 1, \ldots,$ $\nu_\rho - 1$, satisfy

$$\partial_{\xi_1^{(\ell)}}^i \partial_{\xi_2^{(\ell)}}^j \left(f_\ell^{\Gamma^{(\ell+1)}} - f_\ell^{\Gamma^{(\ell)}} \right)(\boldsymbol{0}) = 0, \quad 0 \leq i + j \leq 4, \tag{18}$$

and

$$\partial_{\xi_1^{(\ell)}}^i \partial_{\xi_2^{(\ell)}}^j \left(f_\ell^{\Gamma^{(\ell+1)}} - f_\ell^{\Omega^{(\ell)}} \right)(\boldsymbol{0}) = 0, \quad 0 \leq i, j \leq 2, \tag{19}$$

and in case of a boundary vertex $\boldsymbol{v}^{(\rho)}$, additionally

$$a_{i,j}^{\Gamma^{(0)}} = 0, \ \text{and} \ a_{i,j}^{\Gamma^{(\nu_\rho)}} = 0, \quad 0 \leq i \leq 2, \ 0 \leq j \leq 4 - i. \tag{20}$$

Proof. By (17), the function $\phi_{\boldsymbol{v}^{(\rho)}}$ possesses a support

$$\mathrm{supp}(\phi_{\boldsymbol{v}^{(\rho)}}) \subseteq \cup_{\ell=0}^{\nu_\rho-1} \Omega^{(\ell)}.$$

Equations (18) and (19) ensure that the coefficients $a_{i,j}^{\Gamma^{(\ell)}}$ and $a_{i,j}^{(\ell)}$ are well-defined, which implies that the function $\phi_{\boldsymbol{v}^{(\rho)}}$ is well-defined. The function $\phi_{\boldsymbol{v}^{(\rho)}}$ is now C^2-smooth across the interfaces $\Gamma^{(\ell)}$, since its values, gradients and Hessians along the interfaces $\Gamma^{(\ell)}$ are given by

$$\phi_{\boldsymbol{v}^{(\rho)}}(\Gamma^{(\ell)}) = \sum_{i=0}^{2} \sum_{j=0}^{4-i} a_{i,j}^{\Gamma^{(\ell)}} \, \phi_{\Gamma^{(\ell)};i,j}(\Gamma^{(\ell)}),$$

$$\nabla \phi_{\boldsymbol{v}^{(\rho)}}(\Gamma^{(\ell)}) = \sum_{i=0}^{2} \sum_{j=0}^{4-i} a_{i,j}^{\Gamma^{(\ell)}} \, \nabla \phi_{\Gamma^{(\ell)};i,j}(\Gamma^{(\ell)})$$

and

$$\mathrm{Hess}(\phi_{\boldsymbol{v}^{(\rho)}})(\Gamma^{(\ell)}) = \sum_{i=0}^{2} \sum_{j=0}^{4-i} a_{i,j}^{\Gamma^{(\ell)}} \, \mathrm{Hess}(\phi_{\Gamma^{(\ell)};i,j})(\Gamma^{(\ell)}),$$

respectively, Finally, we obtain $\phi_{\boldsymbol{v}^{(\rho)}} \in \mathcal{V}_{0h}$, since Proposition 1 and equations (20) (in case of a boundary vertex $\boldsymbol{v}^{(\rho)}$) ensure that the function $\phi_{\boldsymbol{v}^{(\rho)}}$ has vanishing values, gradients and Hessians already on the boundary of the multi-patch subdomain $\cup_{\ell=0}^{\nu_\rho-1} \Omega^{(\ell)}$. $\qquad\square$

The equations (18) and (19), and additionally equations (20) in case of a boundary vertex $\boldsymbol{v}^{(\rho)}$, form a homogeneous linear system

$$H^{(\rho)} \boldsymbol{a}^{(\rho)} = \boldsymbol{0}, \tag{21}$$

where $\boldsymbol{a}^{(\rho)}$ is the vector of all involved coefficients $a_{i,j}^{\Gamma^{(\ell)}}$ and $a_{i,j}^{(\ell)}$. Any basis of the null space (i.e., the kernel) of the matrix $H^{(\rho)}$, determines $\dim(\ker H^{(\rho)})$ linearly independent functions $\phi_{\boldsymbol{v}^{(\rho)}} \in \mathcal{V}_{0h}$, which will be denoted by $\phi_{\boldsymbol{v}^{(\rho)};m}$, $m = 1, 2, \ldots, \dim(\ker H^{(\rho)})$. One possible strategy is to find a basis by constructing minimal determining sets (cf. [5, 28]) for the unknown coefficients of the homogeneous linear system (21). In our examples in Section 5, we use the minimal determining set algorithm introduced in [21, Section 6.1] and [20, Section 5.1], which works well and yields well-conditioned functions.

Finally, the vertex subspace $\mathcal{W}_{0h;\boldsymbol{v}^{(\rho)}}$ is defined as

$$\mathcal{W}_{0h;\boldsymbol{v}^{(\rho)}} = \mathrm{span}\{\phi_{\boldsymbol{v}^{(\rho)};m} \mid m = 1, 2, \ldots, \dim(\ker H^{(\rho)})\}.$$

Lemma 4. *We have*

$$\mathcal{W}_{0h;\boldsymbol{v}^{(\rho)}} \subseteq \mathcal{V}_{0h}.$$

Proof. Recall (17). The functions $\phi_{\boldsymbol{v}^{(\rho)};m}$, $m = 1, 2, \ldots, \dim(\ker H^{(\rho)})$, are constructed in such a way that they satisfy $\phi_{\boldsymbol{v}^{(\rho)};m} \in \mathcal{V}_{0h}$. $\qquad\square$

Remark 3. A further possible way for the computation of suitable vertex subspaces could be the extension of the method [18] proposed for the case of C^1-smooth isogeometric functions to our case of C^2-smooth isogeometric functions. In [18], the vertex subspace is defined by globally C^1-smooth functions which are C^2-smooth at the vertex. However, the extension of this approach to our case would require globally C^2-smooth functions which have to be C^4-smooth at the vertex.

4.5. The space $\mathcal{W}_{0h}$

Recall that the space $\mathcal{W}_{0h}$ is the direct sum (14).

Theorem 1. *It holds that*
$$\mathcal{W}_{0h} \subseteq \mathcal{V}_{0h},$$
and the collection of functions
$$\begin{aligned}
\phi_{\Omega^{(\ell)};i,j}, \quad & i,j = 3, 4, \ldots, p + k(p-r) - 3, \ \ell = 1, 2, \ldots, P, \\
\phi_{\Gamma^{(s)};i,j}, \quad & j = 0, 1, \ldots, n_i, \ i = 0, 1, 2, \ s = 1, 2, \ldots, E, \\
\phi_{\boldsymbol{v}^{(\rho)};m}, \quad & m = 1, 2, \ldots, \dim(\ker H^{(\rho)}), \ \rho = 1, 2, \ldots, V,
\end{aligned}$$
forms a basis of the space $\mathcal{W}_{0h}$.

Proof. $\mathcal{W}_{0h} \subseteq \mathcal{V}_{0h}$ is a direct consequence of Lemma 1, 2 and 4, and the definition of the space $\mathcal{W}_{0h}$, see (14). By construction, all functions $\phi_{\Omega^{(\ell)};i,j}$, $\phi_{\Gamma^{(s)};i,j}$ and $\phi_{\boldsymbol{v}^{(\rho)};m}$ are linearly independent, and span the space $\mathcal{W}_{0h}$. $\square$

Remark 4. The functions $\phi_{\Omega^{(\ell)};i,j}$, $\phi_{\Gamma^{(s)};i,j}$ and $\phi_{\boldsymbol{v}^{(\rho)};m}$ are called patch, edge and vertex functions, respectively. All these functions possess a small local support, and are obtained by solving a small system of linear equations and/or by simple explicit formulae. By means of interpolation, the spline functions $\phi_{\Gamma^{(s)};i,j} \circ \boldsymbol{F}^{(\ell)}$ and $\phi_{\boldsymbol{v}^{(\rho)};m} \circ \boldsymbol{F}^{(\ell)}$ can be represented as the spline function $\phi_{\Omega^{(\ell)};i,j} \circ \boldsymbol{F}^{(\ell)}$ with respect to the spline representation (5) (compare e.g., [22]).

Example 1. We consider the three-patch domain (a) visualized in Fig. 7 (first row). The space $\mathcal{W}_{0h}$ is defined as
$$\mathcal{W}_{0h} = \left(\bigoplus_{\ell=1}^{3} \mathcal{W}_{0h;\Omega^{(\ell)}} \right) \oplus \left(\bigoplus_{s=1}^{3} \mathcal{W}_{0h;\Gamma^{(s)}} \right) \oplus \left(\bigoplus_{\rho=1}^{4} \mathcal{W}_{0h;\boldsymbol{v}^{(\rho)}} \right)$$
with the vertices $\boldsymbol{v}^{(1)} = (\frac{17}{3}, 2)$, $\boldsymbol{v}^{(2)} = (\frac{35}{4}, \frac{15}{7})$, $\boldsymbol{v}^{(3)} = (\frac{13}{3}, 4)$ and $\boldsymbol{v}^{(4)} = (5, 0)$, and the edges $\Gamma^{(1)} = \Omega^{(1)} \cap \Omega^{(2)}$, $\Gamma^{(2)} = \Omega^{(2)} \cap \Omega^{(3)}$ and $\Gamma^{(3)} = \Omega^{(3)} \cap \Omega^{(1)}$. For $p = 5$, $r = 2$ and $h = \frac{1}{6}$, the dimensions of the single subspaces are given by
$$\dim \mathcal{W}_{0h;\Omega^{(\ell)}} = 225, \ \dim \mathcal{W}_{0h;\Gamma^{(s)}} = 6, \ \dim \mathcal{W}_{0h;\boldsymbol{v}^{(1)}} = 16 \text{ and } \dim \mathcal{W}_{0h;\boldsymbol{v}^{(\rho)}} = 3,$$
for $s, \ell = 1, 2, 3$ and $\rho = 2, 3, 4$. Furthermore, the functions of the edge space $\mathcal{W}_{0h;\Gamma^{(1)}}$ and the functions of the vertex spaces $\mathcal{W}_{0h;\boldsymbol{v}^{(1)}}$ and $\mathcal{W}_{0h;\boldsymbol{v}^{(2)}}$ are shown in Fig. 5 and Fig. 6, respectively.
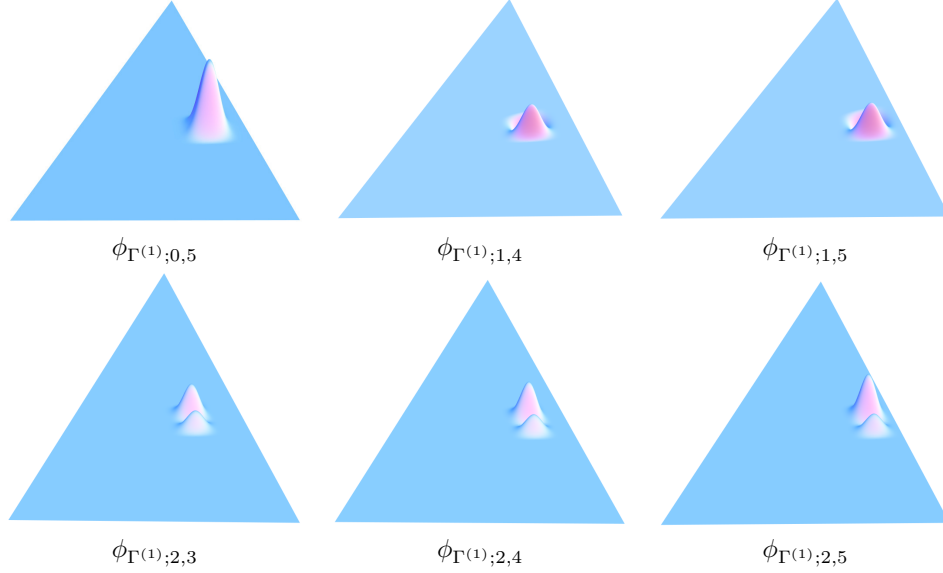
Figure 5: Graphs of the functions of the edge space $\mathcal{W}_{0h;\Gamma^{(1)}}$ for $p = 5$, $r = 2$ and $h = \frac{1}{6}$ (cf. Example 1).

Remark 5. For the sake of simplicity we restricted ourselves to the case of bilinearly parameterized multi-patch domains. The construction of the space $\mathcal{W}_{0h}$ and of its basis should be extendable in a straightforward way to the class of bilinear-like geometries [22]. However, the construction and the study of bilinear-like geometries themselves are limited to the case of two-patch domains [22] so far. But an extension to the case of multi-patch domains is of vital interest for the future research.

5. Solving the triharmonic equation – Examples

We present several examples to demonstrate the potential of our approach for solving the triharmonic equation over bilinear multi-patch domains.

Example 2. We consider the three bilinearly parameterized multi-patch domains given in Figure 7 (first row), which possess extraordinary vertices of valency 3, 5 or 6. For all three domains (a)-(c), we construct nested isogeometric spline spaces $\mathcal{W}_{0h}$ of degree $p = 5$ and regularity $r = 2$ for the mesh-sizes $h = \frac{1}{k+1}$, $k \in \{3, 7, 15, 31\}$. Note that for the case of $h = \frac{1}{4}$, the construction of the space $\mathcal{W}_{0h}$ has to be slightly modified. More precisely, the vertex subspace $\mathcal{W}_{0h;\boldsymbol{v}^{(\rho)}}$ is constructed without the use of the functions $\phi_{\Gamma^{(\ell)};0,4}$. Instead, these functions are added to the corresponding edge subspaces $\mathcal{W}_{0h;\Gamma^{(\ell)}}$ after subtracting suitable linear combinations of functions $\phi_{\Gamma^{(\ell)};i,j}$, $0 \leq i \leq 2$, $0 \leq j \leq \min(4-i, 3)$ to obtain functions $\widehat{\phi}_{\Gamma^{(\ell)};0,4}$ which have vanishing values, gradients and Hessians on $\partial(\Omega^{(\ell-1)} \cup \Omega^{(\ell)})$.

We solve the triharmonic equation (1) with the homogeneous boundary conditions (2) over the domains (a)-(c) for right side functions f obtained by the exact solutions

$$u_a(\boldsymbol{x}) = \left(\frac{1}{20} x_2 \left(\frac{12x_1}{13} - x_2 \right) \left(\frac{120 - 12x_1}{7} - x_2 \right) \right)^3,$$
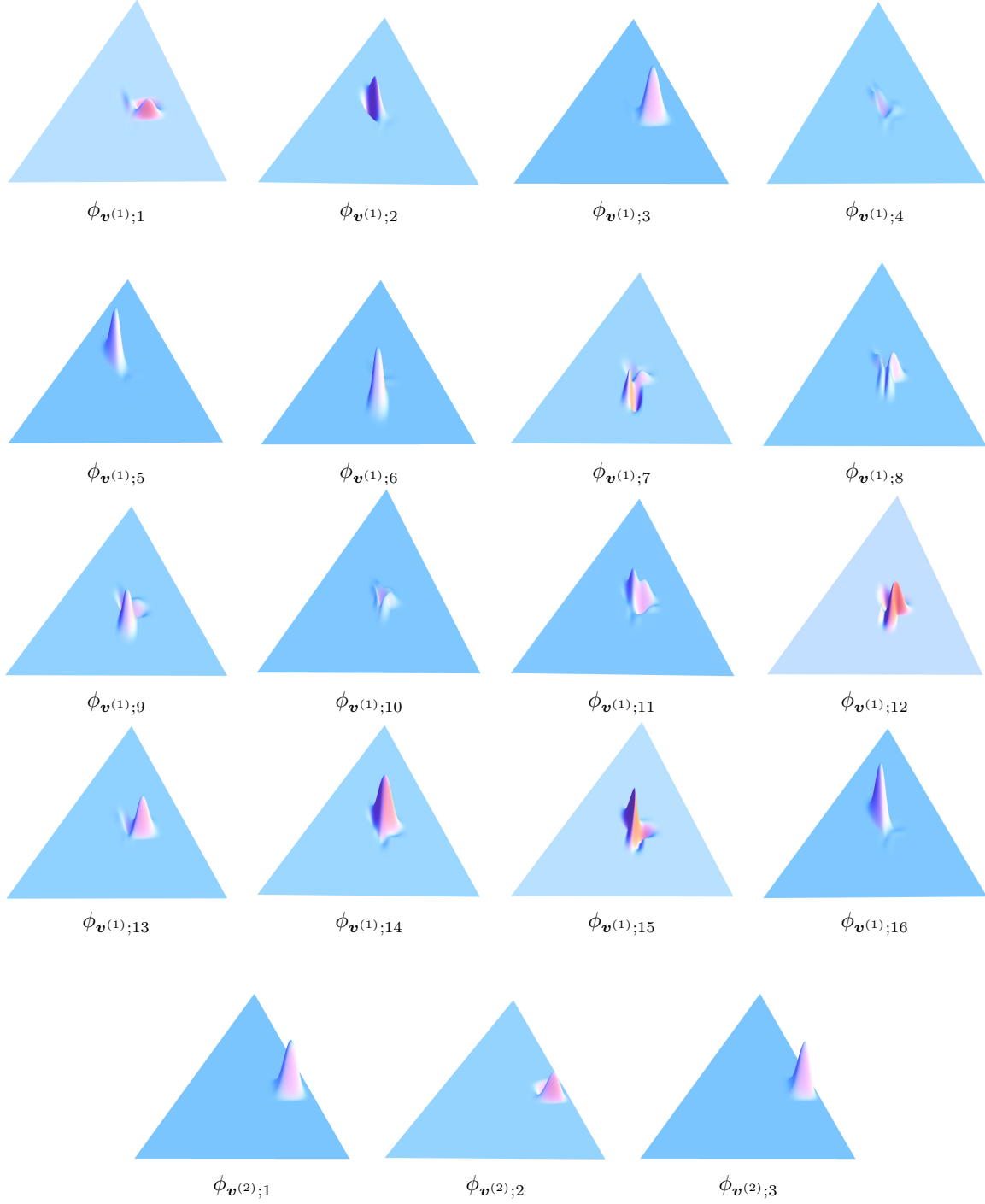
16

Figure 6: Graphs of the functions of the vertex spaces $\mathcal{W}_{0h;\boldsymbol{v}^{(1)}}$ and $\mathcal{W}_{0h;\boldsymbol{v}^{(2)}}$ for $p = 5$, $r = 2$ and $h = \frac{1}{6}$ (cf. Example 1).

$$u_b(\boldsymbol{x}) = \left(\frac{1}{20000}\Big(\frac{121 + 8x_1}{15} - x_2\Big)\Big(\frac{7x_1}{2} + x_2\Big)x_2\Big(\frac{52}{3} - \frac{13x_1}{6} + x_2\Big)\Big(\frac{31}{2} - \frac{9x_1}{11} - x_2\Big)\right)^3$$

and

$$u_c(\boldsymbol{x}) = \left(\frac{1}{200000}\Big(\frac{55 - 5x_1}{2} - x_2\Big)\Big(\frac{1799}{160} - \frac{7x_1}{64} - x_2\Big)\Big(\frac{652 + 78x_1}{61} - x_2\Big)\Big(-\frac{18x_1}{11} - x_2\Big)x_2\Big(\frac{5x_1}{3} - 10 - x_2\Big)\right)^3,$$

see Fig. 7 (second row). The resulting relative H^i-errors, $i = 0, 1, 2, 3$, are visualized in Fig. 7 (third row) and indicate convergence rates of order $\mathcal{O}(h^{6-i})$ in the corresponding norms. [2] Furthermore, Fig. 7 (fourth row) shows the resulting condition numbers κ of the diagonally scaled stiffness matrices S (cf. [7]). The estimated growth rates are of order $\mathcal{O}(h^{-6})$, which demonstrate that the constructed basis functions are well-conditioned.

Example 3. We consider the bilinearly parameterized five-patch domain with four extraordinary vertices of valency 3, which is visualized in Fig. 8 (first row). Analogously to Example 2, nested isogeometric spline spaces $\mathcal{W}_{0h}$ of degree $p = 5$ and regularity $r = 2$ for the mesh-sizes $h = \frac{1}{k+1}$, $k \in \{3, 7, 15, 31\}$, are generated, and are used to solve the triharmonic equation (1) with the homogeneous boundary conditions (2). We use for testing the right side function f which is obtained by the exact solution

$$u(\boldsymbol{x}) = \Big(\frac{1}{20000}x_2\Big(\frac{405}{8} - \frac{27x_1}{8} - x_2\Big)\Big(\frac{425}{38} + \frac{4x_1}{19} - x_2\Big)\Big(\frac{23x_1}{3} - x_2\Big)\Big)^3,$$

see Fig. 8 (first row). Again, the resulting relative H^i-errors are of order $\mathcal{O}(h^{6-i})$, and the estimated growth rates of the diagonally scaled stiffness matrices S are of order $\mathcal{O}(h^{-6})$.

6. Conclusion

We described a method for solving the triharmonic equation over bilinearly parameterized planar multi-patch domains. The presented approach is based on the concept of IGA and uses as discretization space $\mathcal{W}_{0h}$ a space of globally C^2-smooth isogeometric functions. The discretization space $\mathcal{W}_{0h}$ is the span of three different types of test (basis) functions called patch, edge and vertex functions. All of these functions possess a simple representation with small local supports, can be uniformly generated for all possible multi-patch configurations, and are well-conditioned. The numerical results obtained by solving the triharmonic equation over different bilinear multi-patch domains using h-refinement demonstrate the potential of our approach.

The paper leaves several open questions which are worth to study. A first possible topic for future research could be the study of a priori error estimates for the triharmonic equation over multi-patch domains under h-refinement (similar to the ones in [37] for single patch domains), and the theoretical investigation of the approximation properties of the discretization space $\mathcal{W}_{0h}$. Another topic could be the consideration of further 6-th order PDEs for which the use of the discretization space $\mathcal{W}_{0h}$ could be suitable, since these problems require functions of C^2-smoothness. Possible examples are the Kirchhoff

---

[2]Note that for the spaces $\mathcal{W}_{0h}$ the norms $|| \cdot ||_{H^3(\Omega)}$ and $||\nabla \triangle (\cdot)||_{L^2(\Omega)}$ are equivalent.
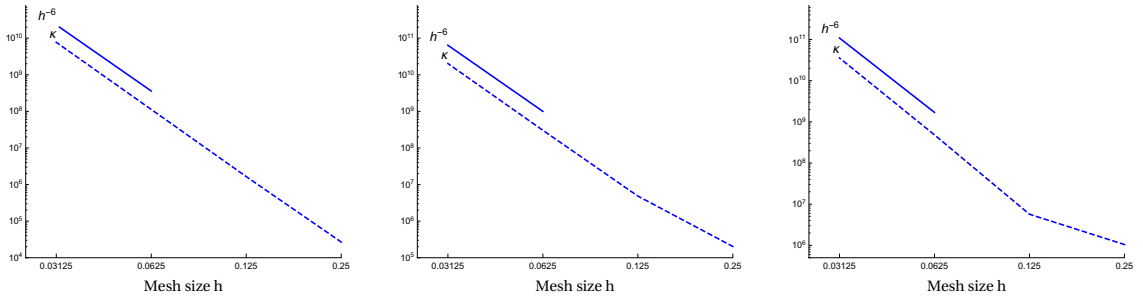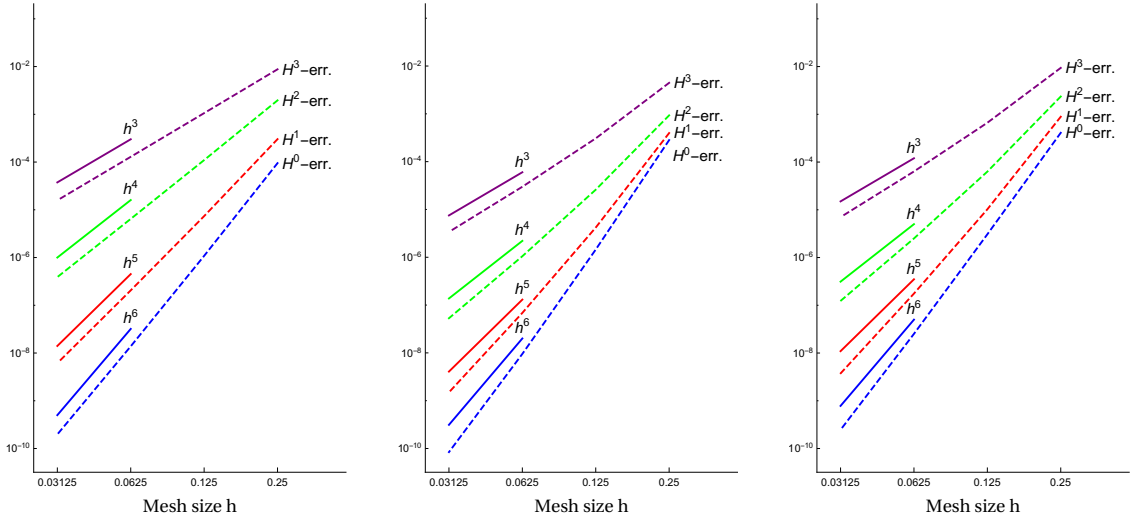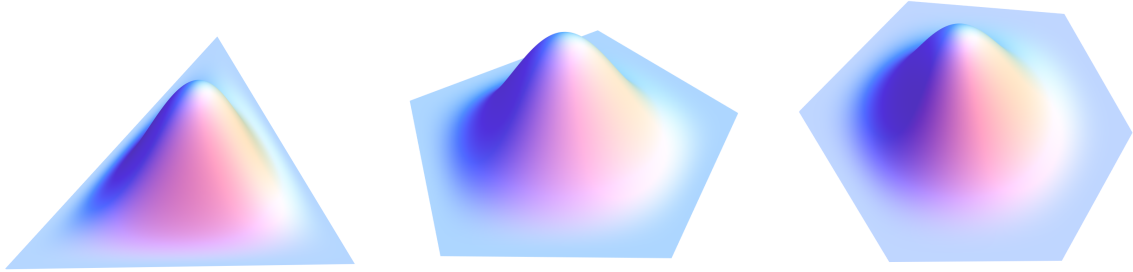
(a)

(b)

(c)

Computational domains Ω

Exact solutions

Relative H^i-errors, $i = 0, \ldots, 3$

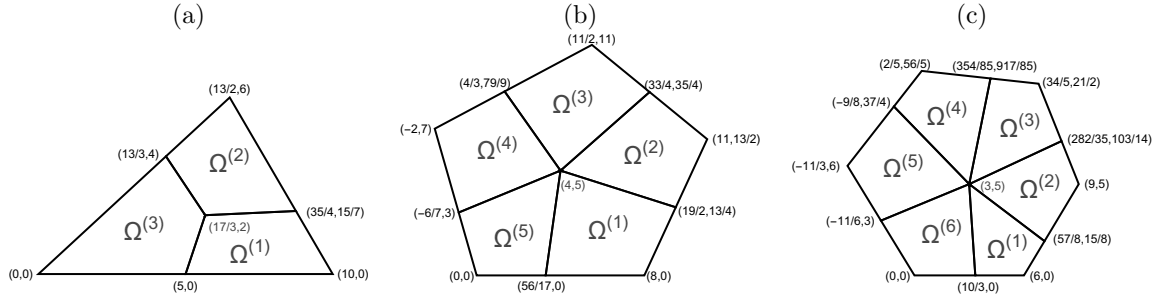Condition numbers κ of the diagonally scaled stiffness matrices S
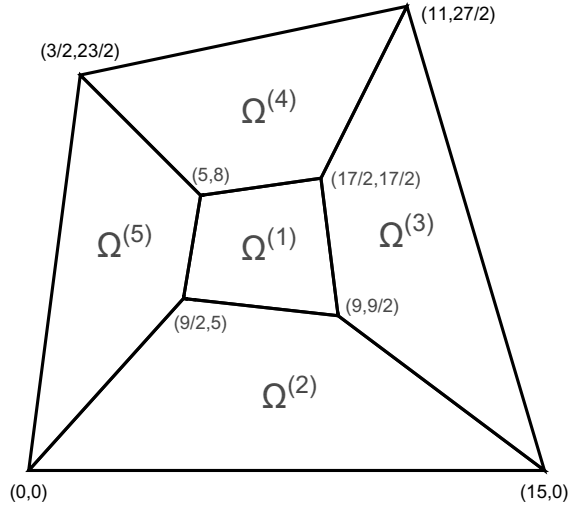
Figure 7: Solving the triharmonic equation over different multi-patch domains Ω (cf. Example 2).

19
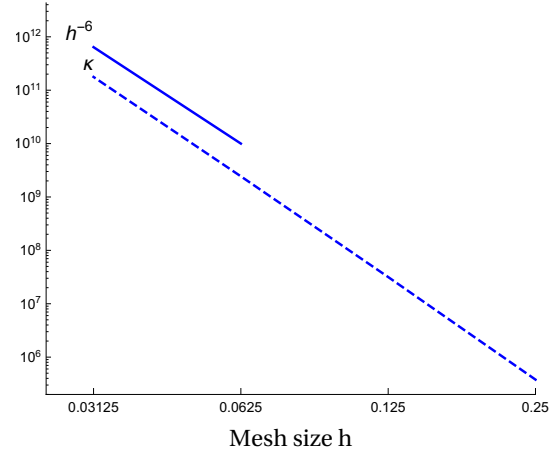
Figure 8: Solving the triharmonic equation over the given multi-patch domain Ω (cf. Example 3).

plate model based on the Mindlin's gradient elasticity theory [33], the Phase-field crystal equation [2, 13] and the gradient-enhanced continuum damage model [41]. The extension of our approach to more general multi-patch domains, such as e.g., bilinear-like planar domains, shells or volumetric domains could be considered, too.

Appendix A. Proof of Proposition 1

The proof will be mainly based on the concept of blossoming. Let $q \in \mathcal{S}_h^{p,r}([0,1])$, and let $t_0^{p,r}, t_1^{p,r}, \ldots, t_{2p+1+k(p-r)}^{p,r}$ be the corresponding knots of the spline space $\mathcal{S}_h^{p,r}([0,1])$. Then there exists a unique function $\mathcal{Q}^{p,r} : \mathbb{R}^d \to \mathbb{R}$, called the *blossom* of q, which is symmetric, multi-affine and fulfill $\mathcal{Q}^{p,r}(\xi, \xi, \ldots, \xi) = q(\xi)$. These properties imply that the control points of q can be written as

$$d_\iota = \mathcal{Q}^{p,r}(t_{\iota+1}^{p,r}, t_{\iota+2}^{p,r}, \ldots, t_{\iota+p}^{p,r}), \quad \iota = 0, 1, \ldots, p + k(p-r).$$

Blossoming is a simple approach, which can be used amongst others to perform knot insertion for a spline function or to multiply two spline functions. For more details about the concept of blossoming we refer to e.g. [10, 35, 36].

The following two lemmas will be needed.

Lemma 5. *Let* $N_j^{p,r+1}(\xi) = \sum_{\iota=0}^{p+k(p-r)} \widetilde{d}_\iota N_\iota^{p,r}(\xi)$. *Then* $\widetilde{d}_\iota = 0$ *for* $\iota < j$.

PROOF. Let d_ι be control points of $N_j^{p,r+1} \in \mathcal{S}_h^{p,r+1}([0,1])$, i.e., $d_\iota = \delta_{j,\iota}$. Moreover let $\widetilde{d}_\iota$ denote control points of $N_j^{p,r+1}$ represented in the space $\mathcal{S}_h^{p,r}([0,1])$. Then (see e.g. [10])

$$\widetilde{d}_\iota = \mathcal{Q}^{p,r+1}(t_{\iota+1}^{p,r}, \ldots, t_{\iota+p}^{p,r}).$$

Since

$$d_\iota = \mathcal{Q}^{p,r+1}(t_{\iota+1}^{p,r+1}, \ldots, t_{\iota+p}^{p,r+1}) \quad \text{and} \quad t_{\iota+p}^{p,r+1} \geq t_{\iota+p}^{p,r},$$

it follows that $\widetilde{d}_\iota = \sum_{m \leq \iota} c_m d_m$, $c_m \in \mathbb{R}$, which implies $\widetilde{d}_\iota = 0$ for $\iota < j$. $\qquad\square$

Lemma 6. *Let* $(\omega_0(1-\xi) + \omega_1\xi) N_j^{p-1,r}(\xi) = \sum_{\iota=0}^{p+k(p-r)} \widehat{d}_\iota N_\iota^{p,r}(\xi)$. *Then* $\widehat{d}_\iota = 0$ *for* $\iota < j$.

PROOF. Let d_ι denote control points of $N_j^{p-1,r} \in \mathcal{S}_h^{p-1,r}([0,1])$, i.e., $d_\iota = \delta_{j,\iota}$, and let $\mathcal{Q}^{p-1,r}$ denote its blossom. Moreover let $\widehat{d}_\iota$ denote the control points of $(\omega_0(1-\xi)+\omega_1\xi) N_j^{p-1,r}(\xi) \in \mathcal{S}_h^{p,r}([0,1])$. Then (see e.g. [10])

$$\widehat{d}_\iota = \frac{1}{p} \sum_{m=1}^{p} \mathcal{Q}^{p-1,r}(t_{\iota+1}^{p,r}, \ldots, t_{\iota+m-1}^{p,r}, t_{\iota+m+1}^{p,r}, \ldots, t_{\iota+p}^{p,r}) (\omega_0(1 - t_{\iota+m}^{p,r}) + \omega_1 t_{\iota+m}^{p,r}).$$

We have to prove that $\widehat{d}_\iota = \sum_{n \leq \iota} c_n d_n$, $c_n \in \mathbb{R}$. Since $d_\iota = \mathcal{Q}^{p-1,r}(t_{\iota+1}^{p-1,r}, \ldots, t_{\iota+p}^{p-1,r})$ and $t_{\iota+p}^{p,r} \leq t_{\iota+p}^{p-1,r}$, it follows that $\mathcal{Q}^{p-1,r}(t_{\iota+1}^{p,r}, \ldots, t_{\iota+m-1}^{p,r}, t_{\iota+m+1}^{p,r}, \ldots, t_{\iota+p}^{p,r})$ does not involve d_n, $n > \iota$. Therefore $\widehat{d}_\iota$ is independent of d_n, $n > \iota$, implying $\widehat{d}_\iota = 0$ for $\iota < j$. $\qquad\square$

Proof of Proposition 1: Recall (12). We first observe that the first summation in (13) follows directly from (10). It remains to prove that the only nonzero coefficients $d^{(\tau)}_{\Gamma^{(s)};m,n}$ might be the ones with $n \geq \max(0, i+j-m)$ and $n \leq \min(d-1, d-n_i+j-i+m)$.

The lower bound follows immediately by using

$$\left(N_j^{p,r}(\xi)\right)' = \sum_{\iota=j-1}^{j} d_\iota \, N_\iota^{p-1,r-1}(\xi), \quad \left(N_j^{p,r}(\xi)\right)'' = \sum_{\iota=j-2}^{j} c_\iota \, N_\iota^{p-2,r-2}(\xi),$$

and by Lemma 5 and Lemma 6. The upper bound can be shown by first considering the function

$$\widehat{g}^{(\tau)}_{\Gamma^{(s)};i,j}(\xi_1^{(\tau)}, \xi_2^{(\tau)}) = g^{(\tau)}_{\Gamma^{(s)};i,n_i-1-j}(\xi_1^{(\tau)}, 1-\xi_2^{(\tau)}),$$

which possesses again the lower bound $n \geq \max(0, i+j-m)$ for possible nonzero coefficients $\widehat{d}^{(\tau)}_{\Gamma^{(s)};m,n}$. This directly implies the upper bound $n \leq \min(d-1, d-n_i+j-i+m)$ for possible nonzero coefficients $d^{(\tau)}_{\Gamma^{(s)};m,n}$ of the function $g^{(\tau)}_{\Gamma^{(s)};i,j}$. $\qquad\square$

References

[1] F. Auricchio, L. Beirão da Veiga, A. Buffa, C. Lovadina, A. Reali, and G. Sangalli. A fully "locking-free" isogeometric approach for plane linear elasticity problems: a stream function formulation. *Comput. Methods Appl. Mech. Engrg.*, 197(1):160–172, 2007.

[2] A. Bartezzaghi, L. Dedè, and A. Quarteroni. Isogeometric analysis of high order partial differential equations on surfaces. *Comput. Methods Appl. Mech. Engrg.*, 295:446 – 469, 2015.

[3] L. Beirão da Veiga, A. Buffa, G. Sangalli, and R. Vázquez. Mathematical analysis of variational isogeometric methods. *Acta Numerica*, 23:157–287, 5 2014.

[4] D. J. Benson, Y. Bazilevs, M.-C. Hsu, and T. J.R. Hughes. A large deformation, rotation-free, isogeometric shell. *Comput. Methods Appl. Mech. Engrg.*, 200(13):1367–1378, 2011.

[5] M. Bercovier and T. Matskewich. *Smooth Bézier Surfaces over Unstructured Quadrilateral Meshes*. Lecture Notes of the Unione Matematica Italiana, Springer, 2017.

[6] A. Blidia, B. Mourrain, and N. Villamizar. G^1-smooth splines on quad meshes with 4-split macro-patch elements. *Comput. Aided Geom. Des.*, 52-53:106 – 125, 2017.

[7] A. M. Bruaset. *A survey of preconditioned iterative methods*, volume 328 of *Pitman Research Notes in Mathematics Series*. Longman Scientific & Technical, Harlow, 1995.

[8] A. Collin, G. Sangalli, and T. Takacs. Analysis-suitable G^1 multi-patch parametrizations for C^1 isogeometric spaces. *Computer Aided Geometric Design*, 47:93 – 113, 2016.

[9] J. A. Cottrell, T.J.R. Hughes, and Y. Bazilevs. *Isogeometric Analysis: Toward Integration of CAD and FEA*. John Wiley & Sons, Chichester, England, 2009.

[10] R. Goldman. *Pyramid algorithms : a dynamic programming approach to curves and surfaces for geometric modeling*. Morgan Kaufmann, San Francisco (Calif.), 2003.

[11] H. Gómez, V. M Calo, Y. Bazilevs, and T. J.R. Hughes. Isogeometric analysis of the Cahn–Hilliard phase-field model. *Comput. Methods Appl. Mech. Engrg.*, 197(49):4333–4352, 2008.

[12] H. Gomez, V. M. Calo, and T. J. R. Hughes. Isogeometric analysis of Phase–Field models: Application to the Cahn–Hilliard equation. In *ECCOMAS Multidisciplinary Jubilee Symposium: New Computational Challenges in Materials, Structures, and Fluids*, pages 1–16. Springer Netherlands, 2009.

[13] H. Gomez and X. Nogueira. An unconditionally energy-stable method for the phase field crystal equation. *Computer Methods in Applied Mechanics and Engineering*, 249 – 252:52 – 61, 2012.

[14] D. Groisser and J. Peters. Matched G^k-constructions always yield C^k-continuous isogeometric elements. *Computer Aided Geometric Design*, 34:67 – 72, 2015.

[15] J. Hoschek and D. Lasser. *Fundamentals of computer aided geometric design*. A K Peters Ltd., Wellesley, MA, 1993.

[16] T. J. R. Hughes, J. A. Cottrell, and Y. Bazilevs. Isogeometric analysis: CAD, finite elements, NURBS, exact geometry and mesh refinement. *Comput. Methods Appl. Mech. Engrg.*, 194(39-41):4135–4195, 2005.

[17] M. Kapl, F. Buchegger, M. Bercovier, and B. Jüttler. Isogeometric analysis with geometrically continuous functions on planar multi-patch geometries. *Comput. Methods Appl. Mech. Engrg.*, 316:209 – 234, 2017.

[18] M. Kapl, G. Sangalli, and T. Takacs. Analysis-suitable C^1 multi-patch isogeometric spaces: basis and dual basis. Technical Report 1711.05161, arXiv.org, 2017.

[19] M. Kapl, G. Sangalli, and T. Takacs. Dimension and basis construction for analysis-suitable G^1 two-patch parameterizations. *Computer Aided Geometric Design*, 52–53:75 – 89, 2017.

[20] M. Kapl and V. Vitrih. Space of C^2-smooth geometrically continuous isogeometric functions on planar multi-patch geometries: Dimension and numerical experiments. *Comput. Math. Appl.*, 73(10):2319–2338, 2017.

[21] M. Kapl and V. Vitrih. Space of C^2-smooth geometrically continuous isogeometric functions on two-patch geometries. *Comput. Math. Appl.*, 73(1):37 – 59, 2017.

[22] M. Kapl and V. Vitrih. Dimension and basis construction for C^2-smooth isogeometric spline spaces over bilinear-like G^2 two-patch parameterizations. *Journal of Computational and Applied Mathematics*, 335:289–311, 2018.

[23] M. Kapl, V. Vitrih, B. Jüttler, and K. Birner. Isogeometric analysis with geometrically continuous functions on two-patch geometries. *Comput. Math. Appl.*, 70(7):1518 – 1538, 2015.

[24] K. Karčiauskas, T. Nguyen, and J. Peters. Generalizing bicubic splines for modeling and IGA with irregular layout. *Computer-Aided Design*, 70:23 – 35, 2016.

[25] J. Kiendl, Y. Bazilevs, M.-C. Hsu, R. Wüchner, and K.-U. Bletzinger. The bending strip method for isogeometric analysis of Kirchhoff-Love shell structures comprised of multiple patches. *Comput. Methods Appl. Mech. Engrg.*, 199(35):2403–2416, 2010.

[26] J. Kiendl, K.-U. Bletzinger, J. Linhard, and R. Wüchner. Isogeometric shell analysis with Kirchhoff-Love elements. *Comput. Methods Appl. Mech. Engrg.*, 198(49):3902–3914, 2009.

[27] J. Kiendl, M.-Ch. Hsu, M. C. H. Wu, and A. Reali. Isogeometric Kirchhoff–Love shell formulations for general hyperelastic materials. *Comput. Methods Appl. Mech. Engrg.*, 291:280 – 303, 2015.

[28] M.-J. Lai and L. L. Schumaker. *Spline functions on triangulations*, volume 110 of *Encyclopedia of Mathematics and its Applications*. Cambridge University Press, Cambridge, 2007.

[29] J. Liu, L. Dedè, J. A. John A Evans, M. J. Borden, and T. J. R. Hughes. Isogeometric analysis of the advective Cahn–Hilliard equation: Spinodal decomposition under shear flow. *Journal of Computational Physics*, 242:321 – 350, 2013.

[30] B. Mourrain, R. Vidunas, and N. Villamizar. Dimension and bases for geometrically continuous splines on surfaces of arbitrary topology. *Computer Aided Geometric Design*, 45:108 – 133, 2016.

[31] T. Nguyen and J. Peters. Refinable C^1 spline elements for irregular quad layout. *Computer Aided Geometric Design*, 43:123 – 130, 2016.

[32] N. Nguyen-Thanh, K. Zhou, X. Zhuang, P. Areias, H. Nguyen-Xuan, Y. Bazilevs, and T. Rabczuk. Isogeometric analysis of large-deformation thin shells using RHT-splines for multiple-patch coupling. *Computer Methods in Applied Mechanics and Engineering*, 316:1157 – 1178, 2017.

[33] J. Niiranen, J. Kiendl, A. H. Niemi, and A. Reali. Isogeometric analysis for sixth-order boundary value problems of gradient-elastic Kirchhoff plates. *Computer Methods in Applied Mechanics and Engineering*, 316:328–348, 2017.

[34] J. Peters. Geometric continuity. In *Handbook of computer aided geometric design*, pages 193–227. North-Holland, Amsterdam, 2002.

[35] L. Ramshaw. Blossoms are polar forms. *Comput. Aided Geom. Des.*, 6(4):323–358, 1989.

[36] H.-P. Seidel. An introduction to polar forms. *IEEE Computer Graphics and Applications*, 13(1):38–46, 1993.

[37] A. Tagliabue, L. Dedè, and A. Quarteroni. Isogeometric analysis and error estimates for high order partial differential equations in fluid dynamics. *Computers & Fluids*, 102:277 – 303, 2014.

[38] D. Toshniwal, H. Speleers, R. Hiemstra, and T. J. R. Hughes. Multi-degree smooth polar splines: A framework for geometric modeling and isogeometric analysis. *Comput. Methods Appl. Mech. Engrg.*, 2016.

[39] D. Toshniwal, H. Speleers, and Hughes T. J. R. Analysis-suitable spline spaces of arbitrary degree on unstructured quadrilateral meshes. Technical Report 16, Institute for Computational Engineering and Sciences (ICES), 2017.

[40] D. Toshniwal, H. Speleers, and Hughes T. J. R. Smooth cubic spline spaces on unstructured quadrilateral meshes with particular emphasis on extraordinary points: Geometric design and isogeometric analysis considerations. *Comput. Methods Appl. Mech. Engrg.*, 327:411–458, 2017.

[41] C. V. Verhoosel, M. A. Scott, T. J. R. Hughes, and R. de Borst. An isogeometric analysis approach to gradient damage models. *Internat. J. Numer. Methods Engrg.*, 86(1):115–134, 2011.

25